Appl Phys A
DOI 10.1007/s00339-011-6702-8

Applied Physics A
Materials Science & Processing

Numerical simulation of process dynamics during laser beam drilling with short pulses

Karl-Heinz Leitz · Holger Koch · Andreas Otto · Michael Schmidt

Received: 26 October 2011 / Accepted: 15 November 2011

Abstract In the last years, laser beam drilling became increasingly important for many technical applications as it allows the contactless production of high quality drill holes. So far, mainly short laser pulses are of industrial relevance, as they offer a good compromise between precision and efficiency and combine high ablation efficiency with low thermal damage of the workpiece. Laser beam drilling in this pulse length range is still a highly thermal process. There are two ablation mechanisms: evaporation and melt expulsion. In order to achieve high quality processing results, a basic process understanding is absolutely necessary. Yet, process observations in laser beam drilling suffer from both the short time scales and the restricted accessibility of the interaction zone. Numerical simulations offer the possibility to acquire additional knowledge of the process as they allow a direct look into the drill hole during the ablation process. In this contribution, a numerical finite volume multi-phase simulation model for laser beam drilling with short laser pulses shall be presented. The model is applied for a basic study of the ablation process with µs and ns laser pulses. The obtained results show good qualitative correspondence with experimental data.

K.-H. Leitz (✉) · H. Koch · M. Schmidt
Chair of Photonic Technologies and Erlangen Graduate School in Advanced Optical Technologies (SAOT), University of Erlangen–Nuremberg, Paul-Gordan-Str. 3, 91052 Erlangen, Germany
e-mail: karl-heinz.leitz@lpt.uni-erlangen.de

A. Otto
Institute for Production Engineering and Laser Technology, Vienna University of Technology, Gusshausstrasse 30, 1040 Vienna, Austria

1 Introduction

Generally, the quality of laser drilled holes gets better with shorter pulse length, mainly due to the reduced formation of melt. However, efficiency decreases as well (see Fig. 1). Single pulse drilling using ms and µs pulses allows the production of many holes within a short time. As there is quite a big amount of melt involved in the process, the quality and reproducibility of the holes is rather low. If higher precision is needed, short and ultrashort pulses in combination with adequate drilling strategies are applied. In this pulse length range, only a small amount of melt is involved in the process, which means that high accuracy can be achieved. However, in the past the medium laser powers of ultrashort-pulsed systems were not sufficient to fulfil industrial efficiency requirements. Besides, studies have shown that even with ultrashort pulses the generation of melt cannot be prevented completely [1–7]. Only recently first attempts for the application of ultrashort laser pulses in industrial production have been reported [8, 9]. However, so far in many industrial applications Q-switched laser systems in the micro- and nanosecond range are still widely common because they can deliver high medium laser power and allow a good compromise between precision and efficiency. As in these processes, there is still a certain amount of melt involved, the choice of the right process parameters and the most suitable drilling strategy is of extreme importance in order to achieve the requested quality [10].

When a laser pulse hits the material, within a short time a multitude of highly dynamic coupled physical processes take place (see Fig. 2). The laser beam is absorbed on the surface of the material, and due to the high intensities of pulsed laser radiation, nearly instantly surface temperatures of some thousand Kelvin are reached, leading to an abrupt evaporation, ionisation of the material and the occurrence of

Published online: 02 December 2011

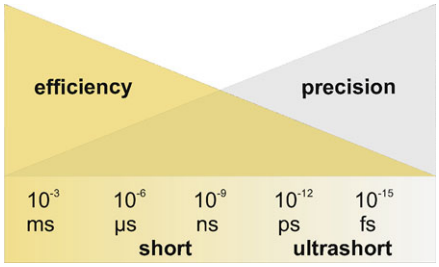

Fig. 1 Influence of the pulse length on precision and efficiency in laser beam drilling

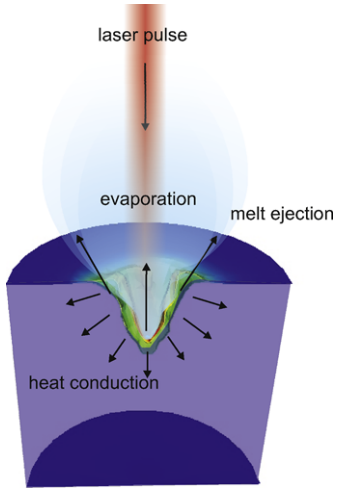

Fig. 2 Beam–matter interaction in laser beam drilling

extreme pressures. The vapour pressure and the expanding effluent vapour lead to an expulsion of the molten material [2, 3, 11, 12].

In order to further optimize the laser beam drilling process, raise the achievable precision and efficiency, a basic process understanding, especially of the mechanisms of spilling and burr formation, is absolutely necessary. This process understanding can be gathered experimentally and theoretically. Experimental in-process approaches deliver information about the temporal dynamics of the laser ablation process [13]. Shadowgraphic and schlieren photography based techniques in combination with high speed imaging can be used to visualize the evolution of the plasma plume and the formation of spillings and shockwaves [14–18]. Post-process approaches use EDX analysis of drilled sandwich sample grindings in order to examine the melt flow within the drill hole [18]. Recently, in-situ imaging of the hole shape evolution during drilling of silicon has been demonstrated using IR transmission imaging [19–21]. All these experimental techniques suffer from the short timescales, the high energy densities and the limited accessibility of the interaction zone.

Numerical simulation models offer the possibility to acquire a deeper understanding of laser beam drilling as they allow a look into the process and principally offer arbitrary spatial and temporal resolution. The first numerical models for laser ablation were restricted to one dimension [22–24] or solely concentrated on heat conduction phenomena [25], as the modelling of melt and vapour dynamics in laser beam drilling is a big numerical challenge because of the extreme physical conditions during and after the impact of the laser pulse [2].

Not until the last years, when cheap and powerful computation power got generally available, the first more or less realistic simulation models for laser beam drilling were developed. Ho et al. presented a computational multi-phase model for heat transfer and gas dynamics in pulsed laser evaporation of metals [26, 27]. They used a finite difference approach for the calculation of temperature distributions, evaporation rate and melting depth in the substrate as well as pressure, velocity and temperature fields in the vapour phase. Ganesh et al. presented a numerical model for laser beam drilling [28, 29] in which the coupled conduction heat transfer in the solid, the advection–diffusion heat transfer in the liquid metal and the fluid dynamics of melt expulsion are modelled for a 2D axisymmetric case. In this model, the melt pool surface is described as a deformable free surface by the volume of fluid approach and a one-dimensional gas dynamics model provides the pressure and temperature on the melt surface. Ruf et al. used several numerical approaches in order to model and investigate the thermo and fluid dynamics in laser beam drilling with short pulses [2]. A commercial finite-element hydrodynamic code FIDAP was used for the simulation of melt formation and dynamics during the impact of a short laser pulse [30]. Temperature and pressure fields were obtained using the hydrodynamic software PARCIPHAL [31]. Dumitru et al. developed a computer model for the laser ablation process taking into account laser absorption, heat diffusion, phase transitions and shielding effects. Based on this model, temporal evolution of drill hole and extension of molten zone could be calculated for single pulses of ns duration [32].

2 Simulation model

In order to study the process dynamics of laser beam drilling at the Chair of Photonic Technologies of the University of Erlangen–Nuremberg, a transient finite volume numerical simulation model was developed utilizing the computational fluid dynamics toolbox OpenFOAM (Open Field Operation And Manipulation, ©OpenCFD Limited). The multi-phase modelling of solid, liquid and gas phase is based on the volume of fluid (VOF) approach [33, 34]. The different phases are treated as incompressible fluids with different viscosities, densities and surface tensions. The fluid dynamics of the multi-phase system is described by a coupled system

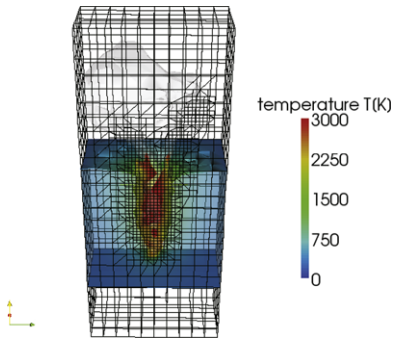

Fig. 3 Adaptive meshing

of three differential transport equations [34–36]. Firstly, one has the continuity equation

$$\frac{\partial \rho}{\partial t} + \nabla \cdot \mathbf{u} = 0 \tag{1}$$

corresponding to the conservation of mass, which states that the mass of a fluid of density ρ can only be changed by a flow with velocity $\mathbf{u}$ across the boundaries. It is closely related to the phase transport equation

$$\frac{\partial \alpha}{\partial t} + \nabla \cdot \alpha \mathbf{u} = 0 \tag{2}$$

with the phase indicator function α whereby $\rho = \sum_i \alpha_i \rho_i$. The second equation is the incompressible Navier–Stokes equation

$$\rho \frac{\partial \mathbf{u}}{\partial t} + \rho \mathbf{u} \cdot \nabla \mathbf{u} = -\nabla p + \rho \mathbf{g} + f_\sigma + \mu \nabla^2 \mathbf{u} \tag{3}$$

with the dynamic viscosity μ, the pressure p, the gravity constant g and the surface tension f_σ, which corresponds to the conservation of impulse and describes the fluid dynamics of the multi-phase system.

The description of the thermal effects during the process is based on the third equation, the equation of heat conduction. As the enthalpies of melting and evaporation play a significant role in the energy balance, they have to be considered. Therefore, an energy-based formulation of the heat conduction equation was chosen taking into account the enthalpies of melting and evaporation [37]:

$$\frac{\partial}{\partial t}(\rho H) + \nabla \cdot (\rho \mathbf{u} H) = \nabla \cdot (\lambda \nabla T) + Q. \tag{4}$$

It includes a convection, conduction and a source term Q describing the energy input of the laser. The equation of heat conduction describes the formation of the temperature field T and corresponds to the conservation of energy [35].

In order to reduce computation time, a symmetry plane was introduced in the model. Furthermore, adaptive meshing was implemented in OpenFOAM. Hereby all cells containing a fraction of melt or vapour different to zero were locally refined. Figure 3 shows the adaptive mesh used for the simulation.

Table 1 Process parameters

Parameter	Symbol	Unit	Value
Medium laser power	P	W	500
Laser wavelength	λ	nm	1064
Pulse frequency	f	s^{-1}	10000
Pulse length	τ	s	$10^{-6}/10^{-9}$
Pulse energy	ϵ	J	0.05
Focus radius	r	µm	50
Sheet thickness	d	mm	0.5

3 Simulation results

The numerical simulation model for beam–matter interaction in laser material processing described in the previous paragraph was applied in order to study the process dynamics of laser beam drilling with short pulses. For this purpose, percussion drilling processes of a 0.5 mm steel sheets were simulated. Hereby pulse durations of 1 µs and 1 ns with identical laser pulse energies were compared to each other. Both spatial and temporal shape of the pulses were of Gaussian shape. Except the pulse duration the other process parameters were exactly the same. They are listed in Table 1.

Figure 4 shows the obtained simulation results for the evolution of the drill hole after 1, 2, 3, 5 and 10 laser pulses of µs and ns duration. The pictures are taken 5 µs after the impact of the laser pulse. Figures 5–10 show the temporal evolution of the drill hole during the first, fifth and tenth laser pulse. The respective time steps were chosen exemplarily in order to show the different phases of the ablation process. The pictures show the interfaces between the solid, liquid and gas phase. The colour corresponds the respective temperature. Vapour material is visualized in transparent white in the gaseous phase.

A comparison of the different pulse durations shows that in an early stage the drilling efficiency of µs pulses is higher, as the energy is used more efficiently. Whereas for ns pulses nearly the complete material is evaporated, for µs pulses the expulsion of molten material significantly contributes the ablation process leading to effective higher ablation rates. In the first phase of the drilling process, ns pulses allow a nearly melt-free ablation, whereas µs pulses lead to a significant melting zone. In a later phase of the drilling process, however, the ablation efficiency of µs pulses decreases as efficiency of melt expulsion drops with increasing depth of the drill hole, whereas it nearly stays constant for ns pulses as the vapour material can still leave deeper drill holes.

This effect can also be observed experimentally. Whereas for µs pulses the increase of drilling depth significantly decreases with the number of laser pulses, ablation efficiency nearly stays constant for ns pulses (see Fig. 11). For deeper holes also for ns pulses a certain amount of melt is involved.

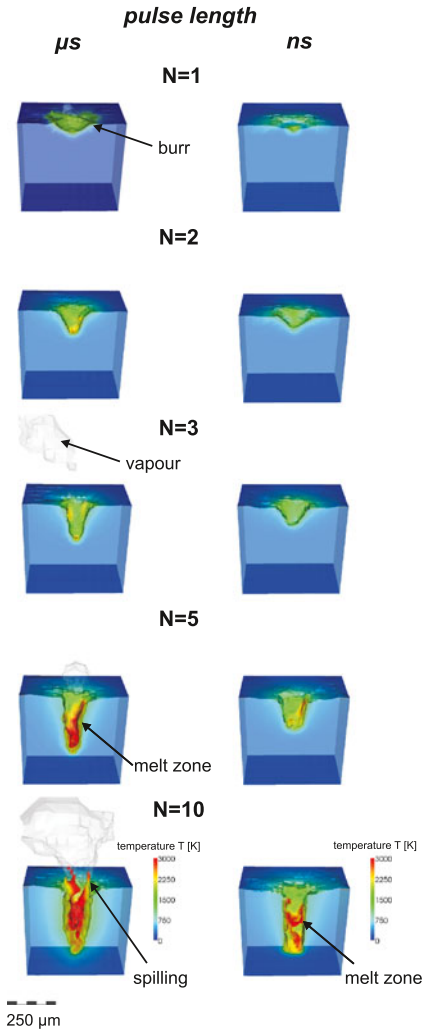

Fig. 4 Drill hole evolution after different numbers of µs and ns laser pulses. The pictures are taken respectively 5 µs after the impact of the laser pulse

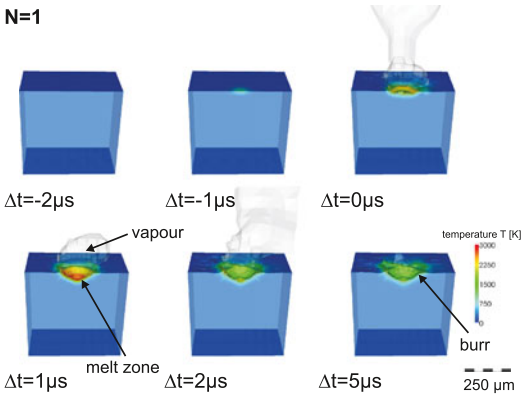

Fig. 5 Drill hole evolution after the first µs laser pulse (Δt time relative to laser pulse)

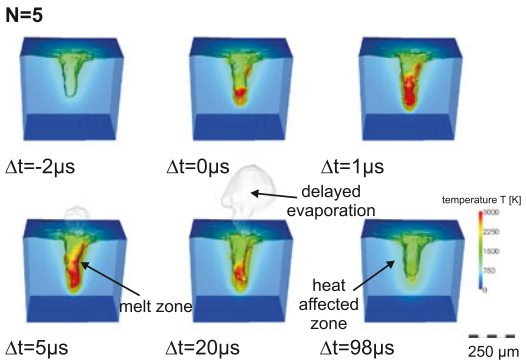

Fig. 6 Drill hole evolution after the fifth µs laser pulse (Δt time relative to laser pulse)

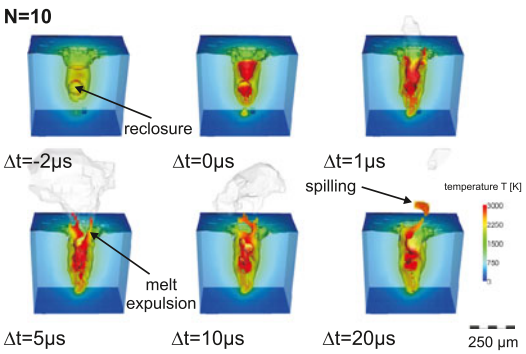

Fig. 7 Drill hole evolution after the tenth µs laser pulse (Δt time relative to laser pulse)

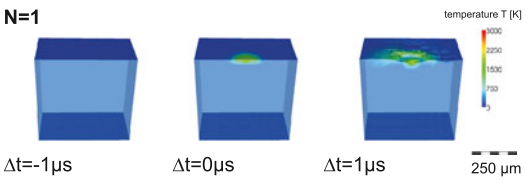

Fig. 8 Drill hole evolution after the first ns laser pulse (Δt time relative to laser pulse)

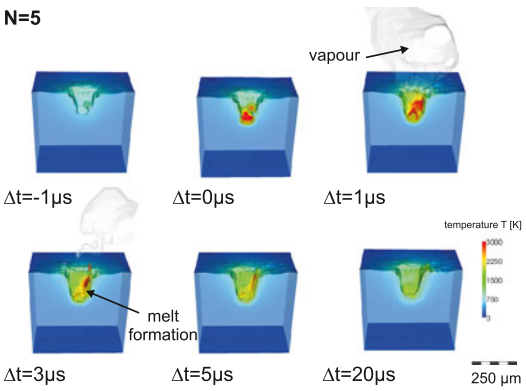

Fig. 9 Drill hole evolution after the fifth ns laser pulse (Δt time relative to laser pulse)

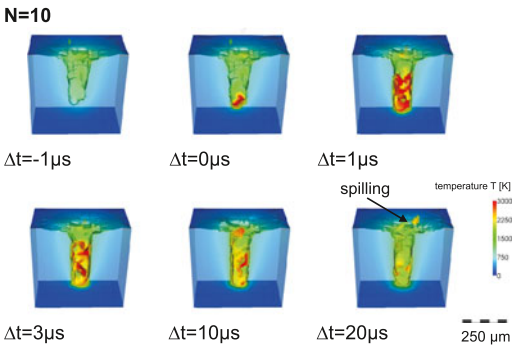

Fig. 10 Drill hole evolution after the tenth ns laser pulse (Δt time relative to laser pulse)

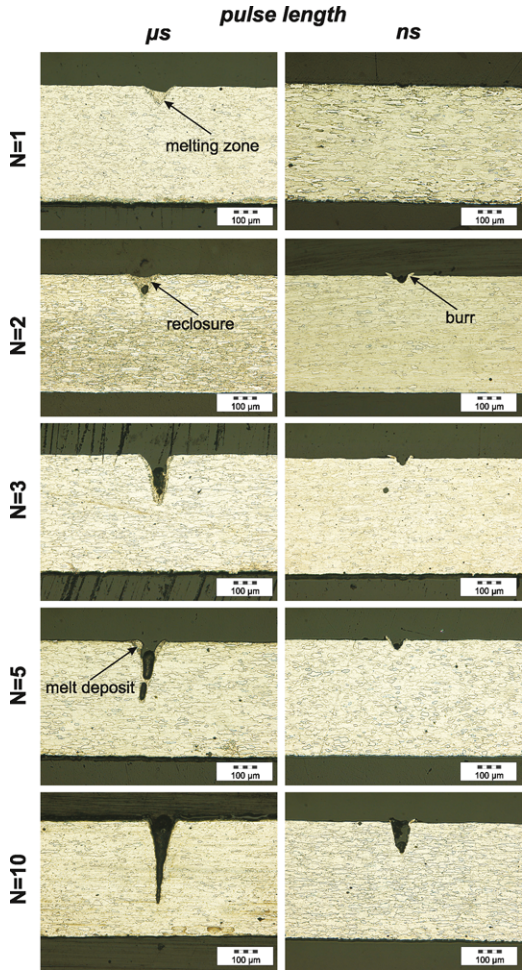

Fig. 11 Grindings of drill holes after different numbers of μs (pulse duration $\tau = 100$ s, wavelength $\lambda = 1064$ nm, pulse energy $\epsilon = 0.06$ J, pulse frequency $f \approx 1$ Hz (hand-trigger)) and ns (pulse duration $\tau = 15$ ns, wavelength $\lambda = 1064$ nm, pulse energy $\epsilon = 0.001$ J, pulse frequency $f = 100$ Hz) drill holes after different numbers of laser pulses

The efficiency of the energy removal drops as the vapour can no longer leave as freely as in an early stage of the drilling process. As a consequence this leads to an enhanced deposition of energy in the drill hole and a subsequent surface melting. Furthermore, with increasing depth of the drill hole the laser pulse hits a bigger area leading to a decreased effective laser intensity.

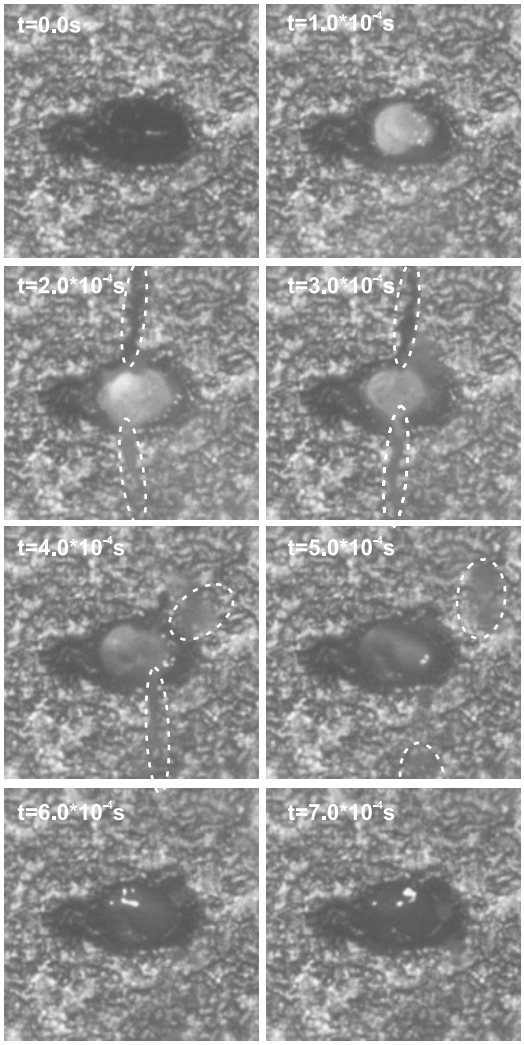

Fig. 12 High speed image series of the impact of a μs laser pulse (pulse duration $\tau = 200$ s, wavelength $\lambda = 1064$ nm, pulse energy $\epsilon = 0.6$ J). Spillings are indicated with *dashed lines*

For both μs and ns pulses, a slight burr formation as well as the formation of spillings can be observed. Both of these effects are more pronounced for μs pulses.

A more detailed look at the temporal dynamics of the process clearly shows the difference between μs and ns laser pulses. Due to the shorter interaction time, there is no vapour 1 μs after the ns pulses whereas for the μs pulse it is still present. Besides μs pulse ablation is accompanied by melt formation and a subsequent thermal influence of the workpiece material (compare Figs. 5 and 8).

In a later phase of the percussion drilling process, other effects become obvious (see Figs. 6 and 9). In this phase, the main ablation mechanism for μs pulses still is evapora-

tion, although there is quite a big amount of melt involved in the process. Part of the material stays molten for up to 100 µs without leaving the drill hole, leading to a significant thermal influence of the workpiece. Furthermore, the simulation shows that evaporation does not stop after the impact of the laser pulse. Due to the huge amount of energy contained in the melt and vapour in the drill hole, evaporation goes on more than 20 µs after the actual impact of the laser pulse. The energy stored in the overheated material leads to an elongated evaporation process (see Fig. 6). For ns pulses the situation is different. The vapour material is immediately transported away, leading to a low thermal influence of the workpiece. Besides the simulation shows that in this drilling phase also for ns pulses a small amount of melt occurs. Yet, the melt has vanished after 20 µs (see Fig. 9). This is in accordance with experimental observations presented in the next section which show that µs pulses lead to a much more pronounced heat affected zone than ns pulses (see Fig. 11).

In a later phase of the drilling process, for µs pulses not all of the molten material resolidifies again. Figure 7 shows the drill hole before the impact of the tenth laser pulse, 98 µs after the impact of the previous. The drill hole is nearly completely filled with melt, showing an enclosed bubble of gas. Observations of similar enclosures were made in grindings of µs pulse series (see Fig. 11). The subsequent impact of the µs laser pulse leads to the expulsion of melt and the formation of spillings. Obviously, in this process phase melt expulsion is a relevant ablation mechanism for µs pulses. The spilling after the tenth µs laser pulse (see Fig. 7) shows a longish shape. Spillings of similar shape were observed in high speed imaging of a µs drilling process (see Fig. 12).

In this later process phase also for ns pulses, a significant amount of melt and spillings can be observed (see Fig. 10). Yet, compared to µs pulses the process is much less thermal. The amount of melt as well as of spillings is much smaller.

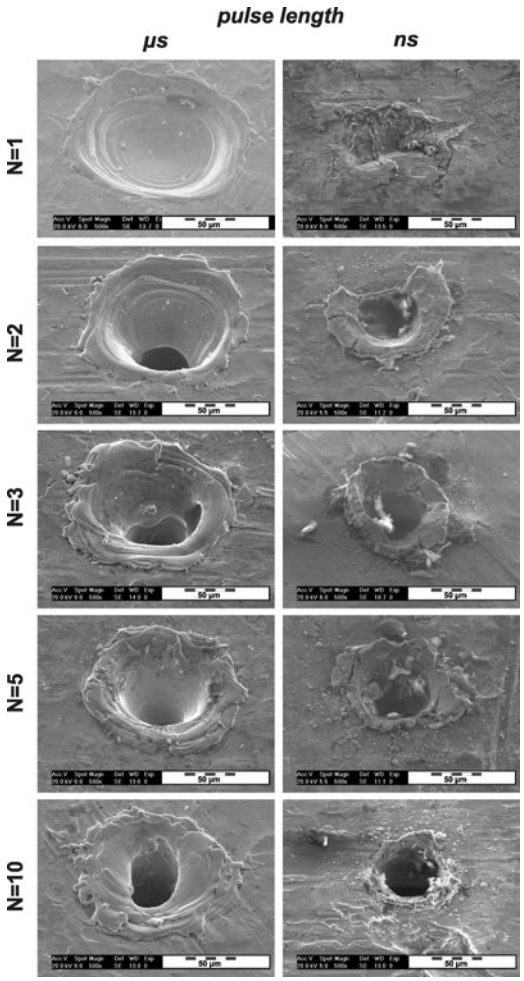

Fig. 13 Scanning electron microscope images of µs (pulse duration $\tau = 100$ µs, wavelength $\lambda = 1064$ nm, pulse energy $\epsilon = 0.06$ J, pulse frequency $f \approx 1$ Hz (hand-trigger)) and ns (pulse duration $\tau = 15$ ns, wavelength $\lambda = 1064$ nm, pulse energy $\epsilon = 0.001$ J, pulse frequency $f = 100$ Hz) drilling holes after different numbers of laser pulses

4 Experimental evaluation

In order to evaluate the numerical simulation model for laser beam drilling, basic experiments with µs and ns laser pulses were performed. For this purpose, steel sheets of 0.5 mm were irradiated with different numbers of µs and ns laser pulses.

Figure 13 shows scanning electron images of drill holes produced with different numbers of µs and ns laser pulses. One can clearly observe that during µs pulse drilling much more melt is involved in the process. The scanning electron images of the µs pulse series show clear melting zones and a significant burr caused by melt swapping over the edge of the drill hole.

Also the ns drill holes show a slight burr, indicating that also in this pulse length range a certain amount of melt is involved. This confirms the results obtained from the numerical simulation model (compare Figs. 9 and 10).

A look at corresponding grindings (see Fig. 11) confirms these observations. The µs pulse drill holes show a clear melting zone. Besides melt ablations in the drill hole, a reclosure of the drill hole can be observed. A similar reclosure of the drill hole could be observed in the numerical simulation (see Fig. 7). The pictures show that for µs pulse drilling melt plays an important role. There are two ablation mechanisms: primary ablation due to evaporation and secondary ablation due to melt expulsion.

For ns pulses, due to the short interaction times and high intensities, melt plays a minor role. The main ablation mechanism is evaporation. There is nearly no melting zone, however, the rough burr that can be seen in the scanning electron microscope images and the grindings shows that melt also plays a role for the ablation process. This result is in accor-

dance with the result obtained from the numerical simulation (compare Figs. 9 and 10).

In order to further investigate the dynamics of short pulse laser drilling, a high speed camera system with a frame rate of 10 kHz and a pulsed diode laser illumination was used to monitor a drilling process with laser pulses of 200 µs (see Fig. 12). Immediately after the impact of the laser pulse, spillings in two different directions occur. Spillings of similar longish shape were also observed in the numerical simulations (see Fig. 7).

5 Conclusions

In this contribution, a numerical simulation model for laser beam drilling with short laser pulses of µs and ns duration was presented. It is able to describe the dynamics of the laser beam drilling process and allows a look into the drill hole with high spatial and temporal resolution. It realistically describes the process of laser ablation with µs and ns pulses by evaporation and melt expulsion. The obtained simulation results show good qualitative correspondence with experimental observations obtained from scanning electron microscope images, metallurgical grindings and high speed imaging.

The model shows that depending on pulse duration and phase of the drilling process different ablation mechanisms are dominant. Depending on the requirements with respect to quality and efficiency, the model can help identify the most suitable beam source and drilling strategy for the respective application.

Acknowledgements The authors gratefully acknowledge funding of the project "Gezielte lokale Sub-100-nm-Strukturierung durch ultrakurze Laserpulse mithilfe von mit einer optischen Pinzette positionierten Kolloiden unter Ausnutzung von Nahfeldeffekten" within the DFG priority programme 1327 "Optisch erzeugte Sub-100-nm Strukturen für biomedizinische und technische Applikationen" and the funding of the Erlangen Graduate School in Advanced Optical Technologies (SAOT) by the German National Science Foundation (DFG) in the framework of the excellence initiative.

References

1. S. Preuss, E. Matthias, M. Stuke, Appl. Phys. A **59** (1994)
2. A. Ruf, *Modellierung des Perkussionsbohrens von Metallen mit kurz- und ultrakurz gepulsten Lasern* (Herbert Utz Verlag, Munich, 2004)
3. F. Dausinger, LTJ Nr. 1 (2004)
4. D. Breitling, A. Ruf, F. Dausinger, Proc. SPIE **5339** (2005)
5. C.Y. Chien, M.C. Gupta, Appl. Phys. A **81** (2005)
6. A. Michalowski, D. Walter, F. Dausinger, J. Laser Micro Nanoeng. **3**(3) (2008)
7. T. Lehecka, A. Mostovych, J. Thomas, Appl. Phys. A **92** (2008)
8. T. Bauer, J. Radtke, J. König, in *Proceedings of the LAMP 2009* (2009)
9. J. König, T. Bauer, Proc. SPIE **7925** (2011)
10. S. Preuss, A. Demchuk, M. Stuke, Appl. Phys. A **61** (1995)
11. M. Dirscherl, *Ultrakurzpulslaser—Grundlagen und Anwendungen* (Bayerisches Laserzentrum, Erlangen, 2005)
12. K.-H. Leitz, H. Koch, A. Otto, M. Schmidt, in *Proceedings of the LIM 2009* (2009)
13. S. Preuss, M. Späth, Y. Zhang, M. Stuke, Appl. Phys. Lett **62**(23) (1993)
14. A. Schoonderbeek, C.A. Biesheuvel, R.M. Hofstra, K.-J. Boller, J. Meijer, Appl. Phys. A **80** (2005)
15. A. Michalowski, D. Walter, P. Berger, F. Dausinger, in *Proceedings of the LIM 2007* (2007)
16. D. Walter, A. Michalowski, R. Gauch, F. Dausinger, in *Proceedings of the LIM 2007* (2007)
17. S. Amoruso, R. Bruzesse, C. Pagano, X. Wang, Appl. Phys. A **89** (2007)
18. A. Michalowski, R. Weber, R. Graf, in *Proceedings of the LIM 2009* (2009)
19. S. Döring, S. Richter, S. Nolte, A. Tünnermann, Opt. Express **19**(18) (2010)
20. S. Döring, S. Richter, S. Nolte, A. Tünnermann, Proc. SPIE **7920** (2011)
21. S. Döring, S. Richter, A. Tünnermann, S. Nolte, Appl. Phys. A **105** (2011)
22. R.G. Evans, A.R. Bell, B.J. MacGowan, J. Phys. D., Appl. Phys. **15** (1982)
23. C.L. Chan, J. Mazumder, J. Appl. Phys. **62**(11) (1987)
24. C.D. Boley, in *International Conference on Applications of Lasers in Electro-Optics* (1994)
25. M.F. Modest, Int. J. Heat Mass Transf. **39**(2) (1996)
26. J.R. Ho, C.P. Grigoropoulos, J.A.C. Humphrey, J. Appl. Phys. **78**(7) (1995)
27. J.R. Ho, C.P. Grigoropoulos, J.A.C. Humphrey, J. Appl. Phys. **79**(9) (1996)
28. R.K. Ganesh, W.W. Bowley, R.R. Bellantone, H. Yukap, J. Comput. Phys. **125** (1996)
29. R.K. Ganesh, A. Faghri, Y. Hahn, Int. J. Heat Mass Transf. **40**(14) (1997)
30. A. Ruf, D. Breitling, P. Berger, F. Dausinger, H. Hügel, Proc. SPIE **4830** (2003)
31. A. Ruf, F. Berger, F. Dausinger, H. Hügel, in *Proceedings of the LIM 2003* (2003)
32. G. Dumitru, V. Romano, H.P. Weber, Appl. Phys. A **79** (2004)
33. C.W. Hirt, B.D. Nichols, J. Comput. Phys. **39** (1981)
34. O. Ubbnik, Numerical prediction of two fluid systems with sharp interfaces, Ph.D. thesis, University of London, 1997
35. J.M. Dowden, *The Mathematics of Thermal Modeling* (Chapman & Hall/CRC, Boca Raton, 2001)
36. M.O. Bristeau, R. Glowinski, J. Priaux, Comput. Phys. Rep. **6** (1987)
37. J.M. Dowden, *The Theory of Laser Material Processing* (Springer, Berlin, 2009)